Case Studies in Thermal Engineering 27 (2021) 101191

Contents lists available at ScienceDirect

Case Studies in Thermal Engineering

journal homepage: www.elsevier.com/locate/csite

Thermal activity of conventional Casson nanoparticles with ramped temperature due to an infinite vertical plate via fractional derivative approach

Ali Raza [a], Sami Ullah Khan [b], Saadia Farid [a], M. Ijaz Khan [c], Tian-Chuan Sun [d,*], Aamar Abbasi [e], M. Imran Khan [f,**], M.Y. Malik [g]

[a] *Department of Mathematics, University of Engineering and Technology, Lahore, 54890, Pakistan*
[b] *Department of Mathematics, COMSATS University Islamabad, Sahiwal, 57000, Pakistan*
[c] *Department of Mathematics and Statistics, Riphah International University I-14, Islamabad, 44000, Pakistan*
[d] *Qiuzhen College, Huzhou University, Huzhou, 313000, PR China*
[e] *Department of Mathematics, University of Azad Jammu & Kashmir, Muzaffarabad, 13100, Pakistan*
[f] *CECOS University of IT & Emerging Sciences, Peshawar, Pakistan*
[g] *Department of Mathematics, College of Sciences, King Khalid University, Abha, 61413, Saudi Arabia*

ARTICLE INFO

Keywords:
Casson nanoparticles
Heat transfer
AB-Fractional derivatives
Analytical solution

ABSTRACT

With inspired thermal characteristics and dynamic applications of nanoparticles, the researchers are motivated to suggest multidisciplinary significances of nano-materials in various thermal engineering and industrial processes. In this analysis, a mixed free convection nanofluid flowing on a vertical plate is discussed with heat transfer in the drilling of nanofluid. The Casson liquid is assumed as a base fluid with uniform suspension of clay nanoparticles. The leading partial differential governing equations with physical properties of nanoparticles are demonstrated with corporal flow phenomenon and imposed thermal conditions. In the governing partial differential equations, the partial derivative with respect to time is replaced by the most recent definition of fractional derivatives i.e. Atangana-Baleanu time-fractional derivative, and then the solution of temperature and velocity field is found by utilizing the Laplace transformation. The effects of different parameters with different values are deliberated and plotted graphically and numerically for temperature and momentum equations. The main results and conclusions are accomplished at the end of this exertion and compared with existing literature. It is concluded that the velocity profile boost up with Grashof number. The results of temperature and momentum equations show a more decaying tendency as compared to Caputo-Fabrizio fractional derivative.

1. Introduction

The study of nanoparticles becomes global and attentive research for scientists in recent times. The nanoparticles reflected increasing dynamic applications in distinct era of engineering, thermal sciences and technological processes. The nanoparticles consist of tiny sized metallic particles having ultra-high thermal performances. The nanoparticles are proffered over base materials as a

* Corresponding author.
** Corresponding author.
E-mail addresses: suntch@zjhu.edu.cn (T.-C. Sun), imrankhan@cecos.edu.pk (M.I. Khan).

https://doi.org/10.1016/j.csite.2021.101191
Received 24 May 2021; Received in revised form 23 June 2021; Accepted 23 June 2021
Available online 26 June 2021

Nomenclatures

v	Velocity$[m/s]$
t	Time$[s]$
U_o	Constant Velocity$[m/s]$
ρ_{nf}	Density of nanofluid$[Kg/m^3]$
T	Non-Dimensional temperature$[K]$
k_{nf}	Thermal conductivity$[W/m^2k]$
γ	Angle of inclination of magnetic field
Pr	Prandtl number
β_c	Casson parameter
Gr	Grashof number
μ_{nf}	Dynamic viscosity$[Kg/ms]$
ρ_s	Density of nanoparticles$[Kg/m^3]$
β	AB-fractional parameter
q	Laplace variable
ρ_f	Density of base fluid$[Kg/m^3]$
g	Acceleration due to gravity$[m/s^2]$

Table 1
Physical characteristics of nanoparticles [4].

Base Fluid/Nanoparticles	$\rho(Kg/m^3)$	$C_p(J/Kg\ K)$	$k(w/m.K)$	$\beta\times10^5(1/K)$
Water	997.1	4179	0.613	21
Kerossene Oil	783	2090	0.145	99
Clay	6320	531.8	76.5	1.80

Table 2
Analysis of Nusselt number Nu with the effect of different parameters.

β	ϕ	t	Nu
0.1	0.00	0.1	1.7462
0.4	0.01	0.1	1.9936
0.7	0.02	0.1	2.6222
0.9	0.03	0.1	3.5763
0.1	0.00	0.3	1.7377
0.4	0.01	0.3	1.8711
0.7	0.02	0.3	2.1403
0.9	0.03	0.3	2.2115
0.1	0.00	0.5	1.7334
0.4	0.01	0.5	1.8028
0.7	0.02	0.5	1.8808
0.9	0.03	0.5	1.9172

resource of energy. With excellent thermo-physical activities, the nanoparticles are attributed as an effective, cheaper and most efficient source of energy. Various chemical processes, metal cutting, thermal systems, machining operations, production processes, heat-flux devices, power pumps etc. The nanoparticles importance is also observed in medical sciences like diagnosis processes, artificial lungs, drug delivery, hyperthermia, heat diseases, cancer treatment etc. The noteworthy properties of nanoparticles were originally reported by Choi [1]. Hsiao [2] inspected the slip features to transport of nanoparticles confining the stagnation point flow. Turkyilmazoglu [3] pointed out the hydromagnetic stability pattern for the single phase nanofluid model. Aman et al. [4] performed analysis for the mass and heat transport of nanoparticles with the numerical simulations. Wakif and Sehaqui [5] suggested the thermal flow for metal oxide nanoparticles for the two-phase flow with convective heating. The nanoparticles optimized flow due to rotating cone has been addressed by Li et al. [6]. Madhukesh et al. [7] focused on the Newtonian heating applications for the AA7072-AA7075/water-based nanoparticles in curved surface. Song et al. [8] determined the thermal improvement in heat transfer by using the Sutterby nanofluid with melting applications. Wakif et al. [9] worked out the meta-analysis for the nanoparticles along with distinct fluid particles movement. Hosseinzadeh et al. [10] addressed the hybrid nanofluid thermal prospective in porous space under the magnetic force influences. Mahanthesh et al. [11] inspected the quadratic convection in nanofluid flow by following two-phase model in presence of dust particles. Salehi et al. [12] examined the squeezing flow of hybrid nanoparticles in parallel plates. Le

Table 3
Analysis of Skin friction$C_f$for the effect of fractional parameter at different time.

β	C_f $t = 1.0$	C_f $t = 1.5$	C_f $t = 2.0$
0.1	0.9853	0.9810	0.9779
0.2	0.9702	0.5226	0.9397
0.3	0.9452	0.9058	0.8756
0.4	0.9063	0.8352	0.7842
0.5	0.8454	0.7373	0.6638
0.6	0.7491	0.6051	0.5149
0.7	0.5980	0.4364	0.3466
0.8	0.3794	0.2473	0.1838
0.9	0.1410	0.0854	0.0567

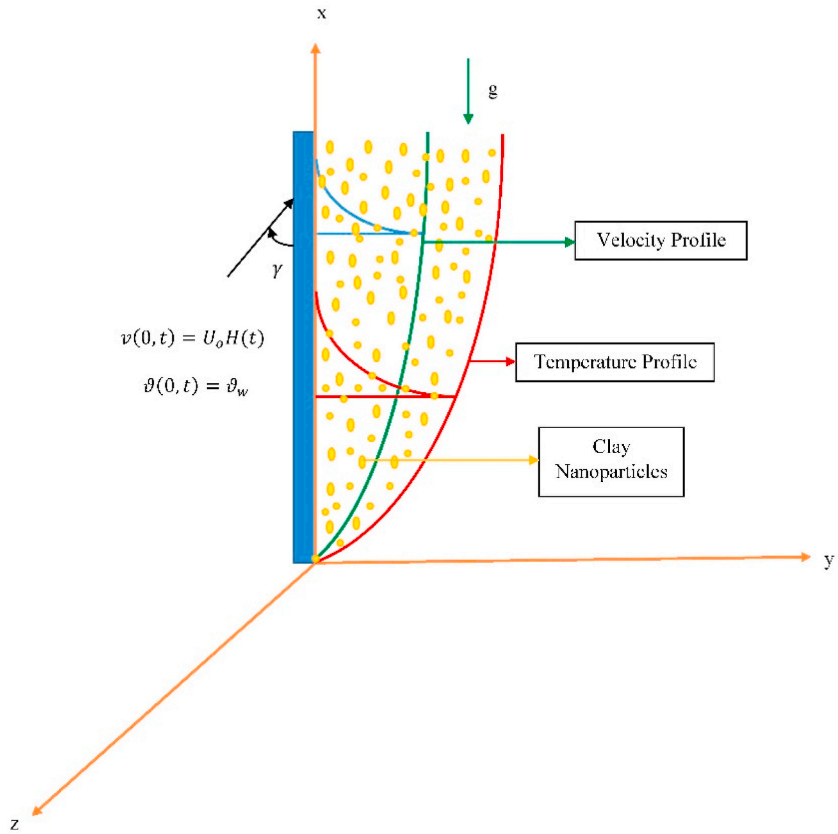

Fig. 1. Physical representation of the problem.

et al. [13] analyzed the thermal prospective of ferrous nanoparticles due to radiated moving cone. Shah et al. [14] discussed the shape pattern of nanoparticles with Lorentz force impact. Saranya and Al-Mdallal [15] presented a computational analysis for the rotating flow of Al_2O_3 nanoparticles with oil base fluid over rotating disk. A three-dimensional Burgers nanofluid with thermal applications was inspected by Khan et al. [16]. Song addressed the thermal properties of ethylene glycol base fluids with alumina and copper nanoparticles. Li et al. [18] visualized the partial slip contributions for the thermal characteristics of hybrid nanoparticles due to spinning disk. (see Tables 1–3)

Due to multidisciplinary nature and interesting rheological dynamics, the analysis regarding the non-Newtonian materials is another interesting research topic. The applications of non-Newtonian fluids in various industries and manufacturing processes make these materials versatile. The novel applications which reflect the non-Newtonian liquids include paint, blood, food processing, cosmetics, gel etc. Moreover, the importance of non-Newtonian fluids is observed in the lubricant industries, cooling/heating processes, oil packaging, opto-electronics and hydraulics. The characterization of such complex materials is strictly depends upon the silent physical consequences. On this end, the properties of non-Newtonian fluids cannot be attributed via implementing the single mathematical relation and model. Scientists have reported different non-Newtonian models in the scientific literature. Casson fluid is classified to the non-Newtonian model due to interesting shear thinning applications. The solid characteristics from Casson fluid are observed when the role of shear force is more dominant as compared to the yield force. The Casson liquid is more applicable the materials with rods a solids and also preferable for accessing the behavior of blood and ink. Khan et al. [19] explored the heat transfer fluctuation in Casson fluid flow by using the thermal radiation effects. Bhatti et al. [20] enrolled the Hall and ion slip applications for the Casson fluid flow subject to the stretched geometry. Kumar et al. [21] obtained the Sakiadis flow results from the Casson fluid flow with three-dimensional configuration. Awais et al. [22] explored the impact of Lorentz force and heat generation for Casson fluid in presence of mass and heat phenomenon. The Casson liquid flow in porous enclosure with radiative phenomenon was analyzed by Rehman et al. [23]. Jamil et al. [24] considered the Casson fluid with application of blood flow by using Caputo-Fabrizio fractional derivatives. Saleem et al. [25] observed the peristaltic motion of Casson liquid with electroosmotic significances. Some studies on different fluid model and flow over a different geometries in mentioned in Refs. [26–31].

This research presents the flow of Casson nanoparticles over a vertical moving plate with help of fractional derivative approach. The enhancement in heat transfer character is inspected with influences of ramped temperature. The solution procedure is followed by using the Atangana-Baleanu time-fractional approach [32–35]. The comparative analysis is performed to verify that analytical simulations. The results are presented for flow parameters with physical explanations.

2. Problem formulation

In this study, we consider a Casson nanofluid flowing on a vertical plate in the xz-plane such that normal to y-axis which is free convection viscous fluid. The incompressible Casson (base) fluid is mixed with clay nanoparticles. Initially, plate and temperature are kept constant. With time $t = 0^+$, the plate begins to move with velocity U_o and temperature increases to T_w. Due to vibrating the plate, the Casson nanofluid also starts to move on the moving plate with the same velocity of the plate as shown in Fig. 1.. The mathematical construction of respective convectional flow can be summarized by the Boussinesq's approximation [32,33] and Rosseland approximation [34] with the following partial differential governing equations [4]:

$$\rho_{nf}\frac{\partial v(\xi,t)}{\partial t}=\mu_{nf}\left(1+\frac{1}{\upsilon}\right)\frac{\partial^2 v(\xi,t)}{\partial \xi^2}+g(\rho\beta)_{nf}[\vartheta(\xi,t)-\vartheta_\infty]Cos(\gamma)\;;\quad \xi,t>0 \tag{1}$$

$$(\rho C_p)_{nf}\frac{\partial\vartheta(\xi,t)}{\partial t}=k_{nf}\frac{\partial^2\vartheta(\xi,t)}{\partial\xi^2}\;;\quad \xi,t>0 \tag{2}$$

with appropriate initial and boundary conditions

$$v(\xi,0)=0,\quad \vartheta(\xi,0)=\vartheta_\infty\quad;\quad \xi>0 \tag{3}$$

$$v(0,t)=U_oH(t),\quad \vartheta(0,t)=\vartheta_w\;;\quad t>0 \tag{4}$$

$$v(\xi,t)\to 0,\quad \vartheta(\xi,t)\to\infty\;;\quad \xi\to\infty,\ t>0 \tag{5}$$

where

$$\rho_{nf}=(1-\phi)\rho_f+\phi\rho_s\,,\quad \mu_{nf}=\frac{\mu_f}{(1-\phi)^{2.5}}$$

$$(\rho\beta)_{nf}=(1-\phi)(\rho\beta)_f+\phi(\rho\beta)_s\,,\quad (\rho C_p)_{nf}=(1-\phi)(\rho C_p)_f+\phi(\rho C_p)_s$$

$$\frac{k_{nf}}{k_f}=\frac{k_s+2k_f-2\phi(k_f-k_s)}{k_s+2k_f+\phi(k_f-k_s)}$$

are the effective density of nanofluid, dynamic viscosity, heat capacitance, the thermal conductivity of nanofluid, and ϕ is the volume fraction of clay nanoparticles.

The suitable dimensionless parameters, to construct the non-dimensional modal, can be indicated as

$$v^*=\frac{v}{v_o}\,,\quad \xi^*=\frac{\xi U_o}{\upsilon_f}\,,\quad t^*=\frac{tU_o^2}{\upsilon_f}\,,\quad T^*=\frac{\vartheta-\vartheta_\infty}{\vartheta_w-\vartheta_\infty}$$

Utilizing these dimensionless parameters and ignoring the star notation, the governing equations (1) and (2) and corresponding conditions can be yields as

$$\left((1-\phi)\rho_f+\phi\frac{\rho_s}{\rho_f}\right)\frac{\partial v(\xi,t)}{\partial t}=\frac{1}{(1-\phi)^{2.5}}\left(1+\frac{1}{\upsilon}\right)\frac{\partial^2 v(\xi,t)}{\partial\xi^2}+\left((1-\phi)+\phi\frac{(\rho\beta)_s}{(\rho\beta)_f}\right)GrT(\xi,t)Cos(\gamma)\;;\quad \xi,t>0 \tag{6}$$

$$\left((1-\phi)+\phi\frac{(\rho C_p)_s}{(\rho C_p)_f}\right)Pr\frac{\partial T(\xi,t)}{\partial t}=\frac{k_{nf}}{k_f}\frac{\partial^2 T(\xi,t)}{\partial\xi^2}\;;\quad \xi,t>0 \tag{7}$$

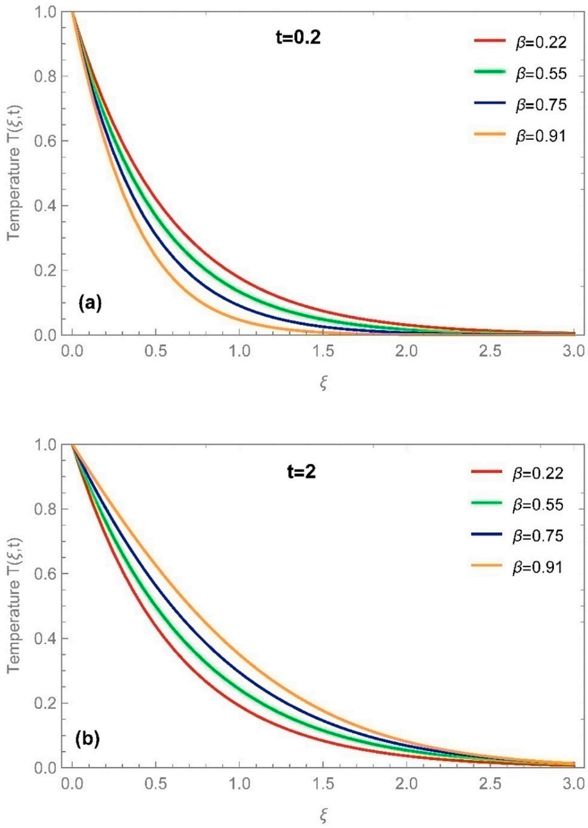

Fig. 2. Variation in fractional constraint for temperature field at **(a)**:$t = 0.2$ and **(b).** $t = 2.0$

with corresponding non-dimensional conditions

$$v(\xi,0)=0, \quad T(\xi,0)=0 \quad ; \quad \xi>0 \tag{8}$$

$$v(0,t)=1, \quad T(0,t)=1 \quad ; \quad t>0 \tag{9}$$

$$v(\xi,t)\rightarrow 0, \quad \vartheta(\xi,t)\rightarrow 0 \quad ; \quad \xi\rightarrow\infty,\ t>0 \tag{10}$$

where $Pr = \frac{\mu_f (C_p)_f}{k_f}$, $Gr = \frac{g\beta_f(\vartheta_w-\vartheta_\infty)}{v_o^3}$are Prandtl and Grashof number respectively.

Definition 1. The Atangana-Baleanu time-fractional derivative can be defined as for the function $f(\xi,t)$

$$^{AB}\mathfrak{D}_t^{\beta} f(\xi,t)=\frac{1}{1-\beta}\int_0^t E_\beta\left[\frac{\beta(t-z)^\beta}{1-\beta}\right]f'_{(\xi,t)}dt; 0<\beta<1 \tag{11}$$

where $^{AB}\mathfrak{D}_t^{\beta}$ is Atangana-Baleanu time-fractional derivative operator with an order of$\beta$and$E_\beta(z)$ is a Mittage-Leffer function which can be expressed as Atangana and Baleanu [35]:

$$E_\beta(z)=\sum_{r=0}^{\infty}\frac{z^\beta}{\Gamma(r\beta+1)}; 0<\beta<1,\ z\in\mathbb{C}$$

Definition 2. The Laplace transformation of the Atangana-Baleanu time-fractional derivative equation (11) can be defined as$^{AB}\mathfrak{D}_t^{\beta}$ is Riaz an dIftikhar [36]:

$$\mathscr{L}\left\{^{AB}\mathfrak{D}_t^{\beta} f(\xi,t)\right\}=\frac{s^\beta\mathscr{L}[f(\xi,t)]-s^{\beta-1}f(\xi,0)}{(1-\beta)s^\beta+\beta} \tag{12}$$

where $s$is the Laplace transformed variable of time t.

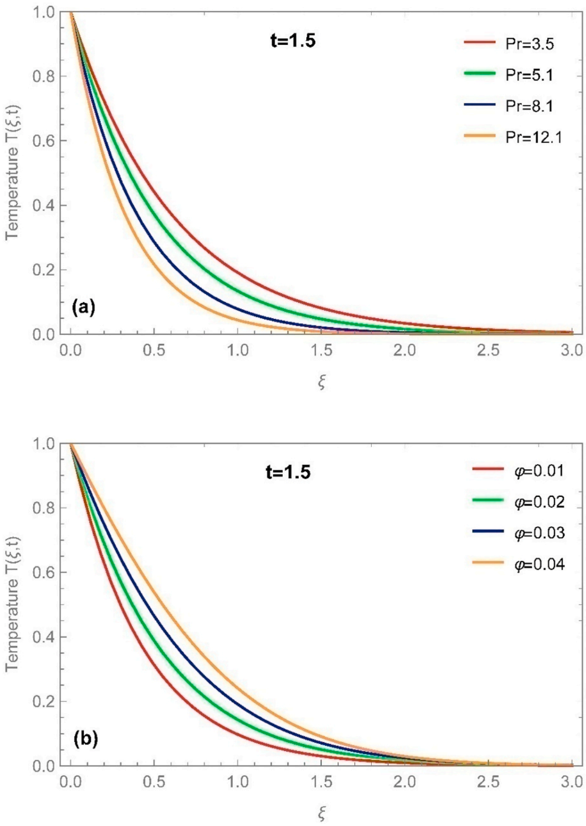

Fig. 3. Variation in **(a):**Prandtl number and **(b):** volume fraction for temperature field at time. $t = 1.5$

3. Modal with Atangana-Baleanu time-fractional derivative

After replacing the ordinary derivative with Atangana-Baleanu time-fractional derivative operator ${}^{AB}\mathfrak{D}_t^{\beta}$of Eqs (6) and (7), we yield the following dimensionless fractional modal

$$\Lambda_1 {}^{AB}\mathfrak{D}_t^{\beta} v(\xi,t) = \Lambda_2 B_c \frac{\partial^2 v(\xi,t)}{\partial \xi^2} + \Lambda_3 Gr T(\xi,t) Cos(\gamma)\ ; \quad \xi, t > 0 \tag{13}$$

$$\Lambda_4 Pr {}^{AB}\mathfrak{D}_t^{\beta} T(\xi,t) = \Lambda_5 \frac{\partial^2 T(\xi,t)}{\partial \xi^2}\ ; \quad \xi, t > 0 \tag{14}$$

where:

$$\Lambda_1 = (1-\phi)\rho_f + \phi \frac{\rho_s}{\rho_f}\ , \quad \Lambda_2 = \frac{1}{(1-\phi)^{2.5}}\ , \quad \Lambda_3 = (1-\phi) + \phi \frac{(\rho\beta)_s}{(\rho\beta)_f}$$

$$\Lambda_4 = (1-\phi) + \phi \frac{(\rho C_p)_s}{(\rho C_p)_f}\ , \quad \Lambda_5 = \frac{k_{nf}}{k_f}\ , \quad \beta_c = 1 + \frac{1}{\upsilon}$$

4. Solution of the problem

4.1. Temperature field

The solution of temperature distribution can originate from the following ordinary differential equation, obtained from transformed equation (14)

$$\Lambda_4 Pr \left(\frac{q^{\beta} \mathscr{L}[T(\xi,t)] - q^{\beta-1} T(\xi,0)}{(1-\beta) q^{\beta} + \beta} \right) = \Lambda_5 \frac{\partial^2 \overline{T}(\xi,q)}{\partial \xi^2} \tag{15}$$

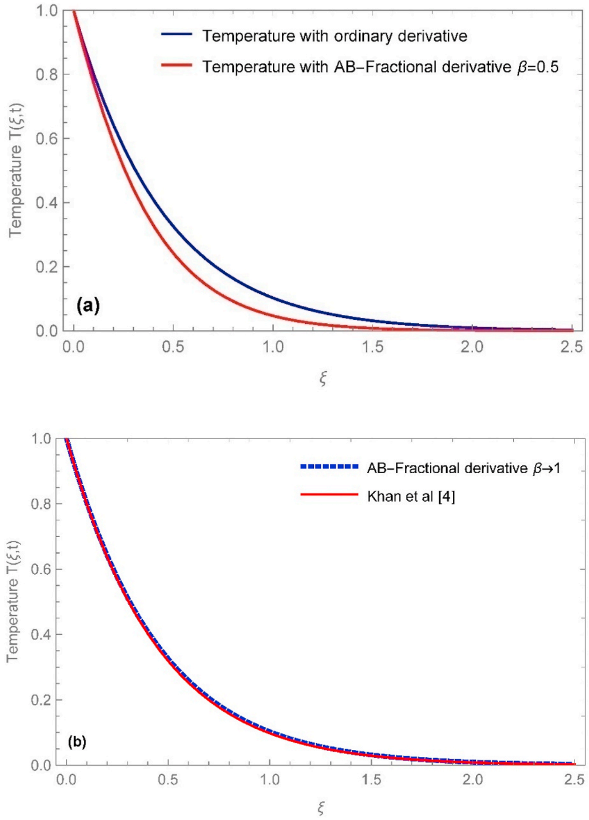

Fig. 4. Comparison for temperature field with fractional and ordinary derivative.

where$\overline{T}(\xi,q)$is the Laplace transformation of$T(\xi,t)$, with the transformed following conditions:

$$\overline{T}(\xi,q)=\frac{1}{q}\ ,\quad \overline{T}(\xi,q)\rightarrow 0\ as\ \xi\rightarrow\infty$$

By utilizing these initial and boundary conditions, we attained the solution of temperature distribution as

$$\overline{T}(\xi,q)=\frac{1}{q}e^{-\xi\sqrt{\frac{\Lambda_4\ Pr}{\Lambda_5}\frac{q^\beta}{(1-\beta)q^\beta+\beta}}} \tag{16}$$

$$\overline{T}_{(\xi,q)}=\overline{\chi}_{(q)}\overline{\psi}_{(\xi,q;a_1,a_2)} \tag{17}$$

where

$$\overline{\chi}_{(q)}=\frac{1}{q^{1-\beta}}\ ,\ \overline{\psi}_{(\xi,q;a_1,a_2)}=\frac{1}{q^\beta}e^{-\xi\sqrt{\frac{a_1\ q^\beta}{q^\beta+a_2}}}\quad ,\quad a_1=\frac{\Lambda_4\ Pr}{\Lambda_5(1-\beta)}\ ,\ a_2=\frac{\beta}{1-\beta}\ ,$$

Now employing the Laplace convolution theorem to find the Laplace inverse of equation (17), which can be inscribed as

$$T_{(\xi,t)}=\int_0^t \chi_{(t-\tau)}\psi_{(\xi,\tau;a_1,a_2)}d\tau\quad ;\quad 0<\beta<1 \tag{18}$$

where:

$$\psi_{(\xi,t;a_1,a_2)}=\mathscr{L}^{-1}\left\{\overline{\psi}_{(\xi,q;a_1,a_2)}\right\}=\frac{1}{\pi}\int_0^\infty\int_0^\infty v\ r^\beta\ Sin(\pi\beta)\psi_{1\ (\xi,t;a_1,a_2)}\ \exp\{-\tau r-vr^\beta Cos(\pi\beta)\}drdu$$

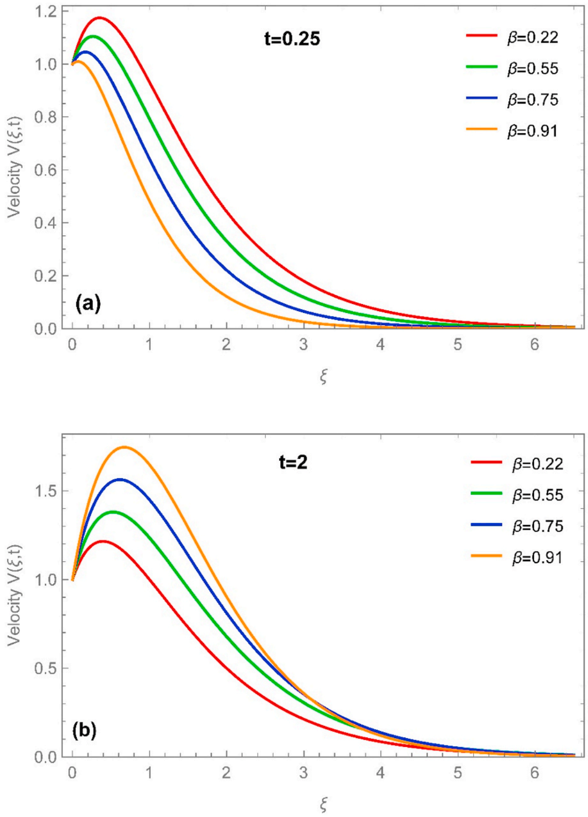

Fig. 5. Variation in fractional constraint for velocity field at **(a)**:$t = 0.25$ and **(b).** $t = 2.0$

$$\psi_{1\,(\xi,t;a_1,a_2)} = \mathscr{L}^{-1}\left\{\frac{1}{q}e^{-\xi\sqrt{\frac{a_1\,q}{q+a_2}}}\right\} = 1 - \frac{2\,a_1}{\pi}\int_0^\infty \frac{Sin(\xi x)}{x(a_1+x^2)}e^{-\frac{a_2 t x^2}{a_1+x^2}}\,dx \tag{19}$$

and

$$\chi_{(t)} = \frac{t^{-\beta}}{\text{Gamma}(1-\beta)}$$

where $H(t)$ is the Heaviside function and also noticed equation (18) will satisfy all imposed physical conditions that satisfy this solution.

4.2. Velocity field

Eq (13) is a partial differential equation of AB-fractional modal and can be transformed into an ordinary derivative by applying the Laplace transformation and utilizing the result Eq (12)

$$\Lambda_1\left(\frac{q^\beta \mathscr{L}[v(\xi,t)] - q^{\beta-1}v(\xi,0)}{(1-\beta)q^\beta+\beta}\right) = \Lambda_2\beta_c\frac{\partial^2\overline{v}(\xi,q)}{\partial\xi^2} + \Lambda_3 Gr\overline{T}(\xi,q)Cos(\gamma)\,; \quad \xi > 0 \tag{20}$$

with the following transformed initial and boundary conditions

$$\overline{v}(0,q) = 0 \; and \quad \overline{v}(\xi,q) \to 0 \; as \; \xi \to \infty \tag{21}$$

The solution of Eq (20) by using conditions (21) is obtained as

$$\overline{v}(\xi,q) = \frac{1}{q}e^{-\xi\sqrt{\frac{\Lambda_1}{\Lambda_2 B_c}\frac{q^\beta}{(1-\beta)q^\beta+\beta}}} + \frac{\Lambda_3\;GrCos(\gamma)}{q^{1+\beta}}\frac{(1-\beta)q^\beta+\beta}{\frac{\Lambda_4\;Pr}{\Lambda_5}-\frac{\Lambda_1}{\Lambda_2 B_c}}\left(e^{-\xi\sqrt{\frac{\Lambda_1}{\Lambda_2 B_c}\frac{q^\beta}{(1-\beta)q^\beta+\beta}}} - e^{-\xi\sqrt{\frac{\Lambda_4\;Pr}{\Lambda_5}\frac{q^\beta}{(1-\beta)q^\beta+\beta}}}\right) \tag{22}$$

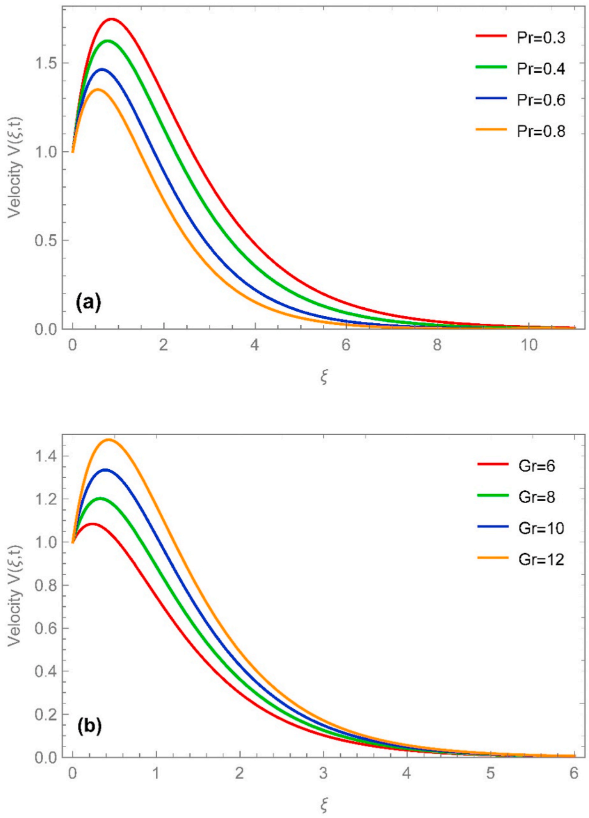

Fig. 6. Variation in **(a):**Prandtl number and **(b):**Grashof number for velocity profile.

The inverse of Laplace for the velocity field of Eq (22), we will use the Grave Stehfest and Zakians method with mathematical form as [7–9]:

$$u(\xi,t)=\frac{ln(2)}{t}\sum_{n=1}^{M}v_n\overline{u}\left(\xi,n\frac{ln(2)}{t}\right)$$

where M will be a positive integer, and

$$v_n=(-1)^{n+\frac{M}{2}}\sum_{p=\frac{q+1}{2}}^{min\left(q,\frac{M}{2}\right)}\frac{p^{\frac{M}{2}}(2p)!}{\left(\frac{M}{2}-p\right)!p!\,(p-1)!\,(q-p)!\,(2p-q)!}$$

and

$$u(\xi,t)=\frac{2}{t}\sum_{j=1}^{N}Re\left(k_j\,.\,\overline{u}\left(\xi,\frac{\alpha_j}{t}\right)\right)$$

5. Results and discussion

The model presents the thermal applications of Casson nanoparticles with help of fractional derivatives with Atnagana-Baleanu time-fractional derivative. The suspension of clay nanoparticles is considered with Casson as a base fluid for the temperature and velocity profile. The solution of partial differential governing equations i.e. temperature and velocity field is analyzed by utilizing Laplace transformation. The behavior of different parameters on temperature and velocity profile is analyzed graphically by using math software Mathematica. The effects of fractional parameter β on the temperature distribution are analyzed in Fig. 2 (a) and (b) for different values of the fractional parameter and at different values of time t. A fascinating behavior of temperature profile for different values of time is observed that temperature decays for small values of time then increases by increasing the value of time. In Fig. 3 (a-b) Fig. 4 (a)-(b) the effects of Prandtl number Pr and volume fraction ϕ on temperature distribution are displayed respectively. The

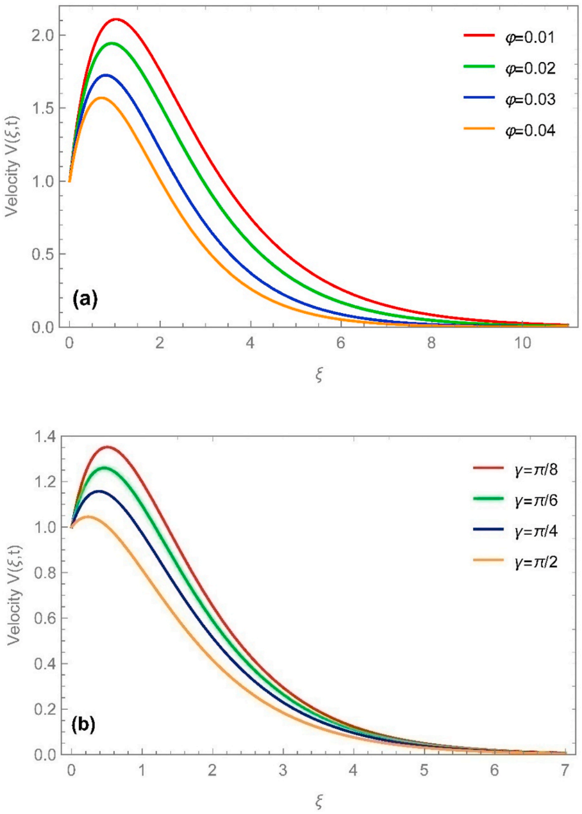

Fig. 7. Variation in **(a):** Volume fraction and **(b):** direction of magnetic field for velocity profile.

enhancement in the value of *Pr* decreases the thermal conductivity of the fluid that's why the temperature of the nanofluid decreases by increasing the value of *Pr* and the thermal conductivity of the fluid increases by increasing the volume fraction that's why temperature also increases by increasing the value of volume fraction ϕ. The comparison of temperature for the fractional and ordinary derivative is highlighted in Fig. 4 (a) and the comparison of our study with existing literature is highlighted in Fig. 4 (b). It can be seen in Fig. 4(a) that the Casson fluid has a more decaying behavior for fractional derivative as compared to ordinary derivative for temperature while it overlaps on ordinary derivative when the value of fractional parameter tends to $\beta \rightarrow 1$ in Fig. 4(b).

The behavior of the velocity profile for the fractional constraint is presented in Fig. 5(a)-(b) which has also dual behavior for different values of the time. In Fig. 6 (a)-(b) the effects of Prandtl number *Pr* and Grashof *Gr* are bright into the light for velocity profile respectively. Increases in Prandtl number means an increase in viscosity which creates some resistance in the flow of fluid and fluid velocity decreases by increasing the value of Prandtl number while increases in Grashof number tends to increases in buoyancy effect which increases the fluid velocity, as shown in Fig. 6 (a)–(b) respectively. The effects of volume fraction ϕ and the inclination of magnetic field γ on the velocity field are plotted in Fig. 7 (a)-(b) and observed that by enhancing the value of volume fraction of nanoparticles increases the viscous effect of nanofluid which decreases the velocity of clay-based nanoparticles fluid and increase in the inclination angle of the magnetic field decreases the nanofluids velocity, as shown in Fig. 7 (a)–(b) respectively. Finally, the comparison of fractional and ordinary with viscous and Casson fluid for the velocity field and the comparison of our study velocity via Atangana-Baleanu time-fractional derivative is compared with the existing literature in Fig. 8 (a) and (b) respectively for the changed values of fractional constraint β. It can be noted in Fig. 8 (a) and (b) that the fractional nanofluid decays as compared to ordinary nanofluid for both viscous and Casson nanofluid, and the comparison of the obtained velocity profile via Atangana-Baleanu time-fractional derivative with existing literature is displayed in Fig. 8(b) which ovelaps to ordinary derivative curve for $\beta \rightarrow 1$. From the graphical representation of temperature and velocity profile, it can be concluded that the results obtained from Atangana-Baleanu time-fractional derivative show more decaying behavior as compared to the Caputo-fractional derivative.

6. Conclusions

The thermal applications of Casson nanoparticles due to infinite vertical surface are presented with help of fractional derivative approach. The Atangana-Baleanu time-fractional derivative approach is followed to present the solution of formulated problem. Moreover, the numerical outcomes for thermal flow problem are presented with the help of Laplace transformation. The novel observations are summarized as.

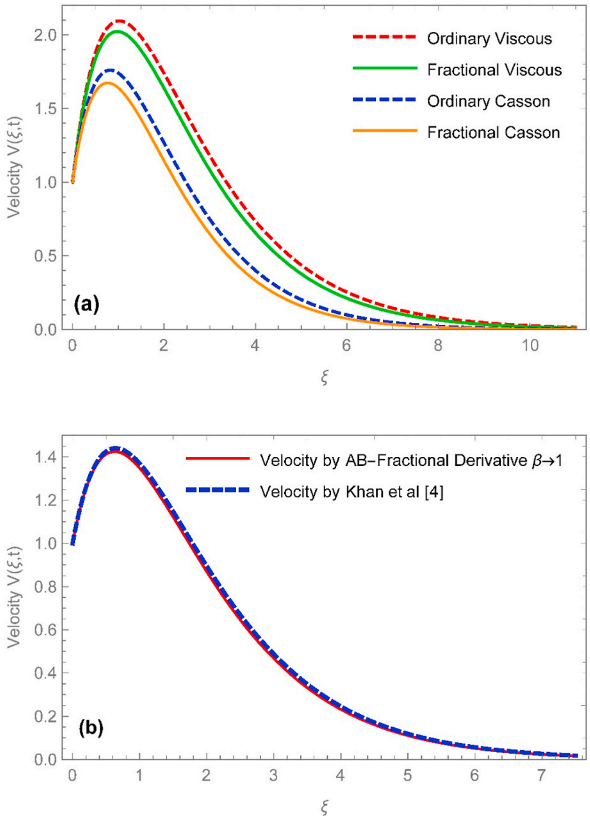

Fig. 8. Comparison of velocity profile with **(a):** Viscous and Casson fluid **(b):** fractional with ordinary velocity.

- ➢ A decaying change in the velocity and nanoparticles temperature is observed for Atangana-Baleanu time-fractional derivative as compared to ordinary derivative.
- ➢ The temperature field decays by enhancing the value of Pr while it shows an increasing behavior for volume fraction ϕ.
- ➢ The velocity field increases when enhancing the value ofGrashof number Gr and shows dual behavior for fractional constraint β for different values of the time.
- ➢ By enhancing the values of Prandtl number Pr and volume fraction ϕ, the velocity profile decreases.
- ➢ For the Casson fluid for both cases fractional and ordinary velocity field decreases as compared to viscous fluid.

Author statement

This work is done under the supervision of Dr. M. Ijaz Khan. The authors Ali Raza and M. Imran Khan provide the conceptualization and validation of the results, the authors Saadia Farid and Sami Ullah Khan have prepared the original draft, the authors Tian-Chuan Sun, Aamar Abbasiand M. Y. Malik have plot the result through software and review and edit the final draft.

Declaration of competing interest

The authors declare that they have no known competing financial interests or personal relationships that could have appeared to influence the work reported in this paper.

Acknowledgement

The authors extend their appreciation to the Deanship of Scientific Research at King Khalid University, Abha 61413, Saudi Arabia for funding this work through research groups program under grant number R.G.P-1/234/42.

References

[1] S.U.S. Choi, Enhancing thermal conductivity of fluids with nanoparticles, ASME Pub. Fed. 231 (1995) 99–106.
[2] Kai-Long Hsiao, Stagnation electrical MHD nanofluid mixed convection with slip boundary on a stretching sheet, Appl. Therm. Eng. 98 (2016) 850–861.

[3] M. Turkyilmazoglu, Single phase nanofluids in fluid mechanics and their hydrodynamic linear stability analysis, Computer Methods and Programs in Biomedicine, Computer Methods and Programs in Biomedicine, Available online 3 November 2019, 105171.
[4] S. Aman, I. Khan, Z. Ismail, M.Z. Salleh, Applications of fractional derivatives to nanofluids: exact and numerical solutions, Math. Model Nat. Phenom. 13 (1) (2018) 2.
[5] Abderrahim Wakif, Rachid Sehaqui, Generalized differential quadrature scrutinization of an advanced MHD stability problem concerned water-based nanofluids with metal/metal oxide nanomaterials: a proper application of the revised two-phase nanofluid model with convective heating and through-flow boundary conditions, Numerical Methods for Partial Differential Equations, https://doi.org/10.1002/num.22671.
[6] Yong-Min Li, M. Ijaz Khan, Sohail A. Khan, Sami Ullah Khan, Zahir Shah, Poom Kumam, an assessment of the mathematical model for estimating of entropy optimized viscous fluid flow towards a rotating cone surface, Sci. Rep. 11 (2021). Article number: 10259.
[7] J.K. Madhukesh, R. Naveen Kumar, R.J. Punith Gowda, B.C. Prasannakumara, G.K. Ramesh, Sami Ullah Khan, Yu-Ming Chu, Numerical simulation of AA7072-AA7075/water-based hybrid nanofluid flow over a curved stretching sheet with Newtonian heating: a non-Fourier heat flux model approach, J. Mol. Liq. 335 (2021) 116103, 1 August.
[8] Ying-Qing Song, Waqas Hassan, Kamel Al-Khaled, Umar Farooq, Sami Ullah Khan, M. Ijaz Khan, Yu-Ming Chu, Sumaira Qayyum, Bioconvection analysis for Sutterby nanofluid over an axially stretched cylinder with melting heat transfer and variable thermal features: a Marangoni and solutal model, Alexandria Engineering Journal 60 (5) (October 2021) 4663–4675.
[9] A. Wakif, I.L. Animasaun, P.V. Satya Narayana, G. Sarojamma, Meta-analysis on thermo-migration of tiny/nano-sized particles in the motion of various fluids, Chin. J. Phys. 68 (2020) 293–307. December.
[10] Kh Hosseinzadeh, So Roghani, A.R. Mogharrebi, A. Asadi&D, D. Ganji, Optimization of hybrid nanoparticles with mixture fluid flow in an octagonal porous medium by effect of radiation and magnetic field, J. Therm. Anal. Calorim. 143 (2021) 1413–1424.
[11] B. Mahanthesh, Joby Mackolil, M. Radhika, Wael Al-Kouz, Siddabasappa, Significance of quadratic thermal radiation and quadratic convection on boundary layer two-phase flow of a dusty nanoliquid past a vertical plate, Int. Commun. Heat Mass Tran. 120 (January 2021) 105029.
[12] Sajad Salehi, Amin Nori, Kh Hosseinzadeh, D.D. Ganji, Hydrothermal analysis of MHD squeezing mixture fluid suspended by hybrid nanoparticles between two parallel plates, Case Studies in Thermal Engineering 21 (October 2020) 100650.
[13] HuGe-Ji Le, Nehad Ali Shah, Y.M. Mahrous, Pooja Sharma, C.S.K. Raju, S. Mamatha Upddhya, Radiated magnetic flow in a suspension of ferrous nanoparticles over a cone with brownian motion and thermophoresis, Case Studies in Thermal Engineering 25 (June 2021) 100915.
[14] Zahir Shah, Ikramullah, Poom Kumam, Mahmoud M. Selim, Alshehri Ahmed, Impact of nanoparticles shape and radiation on the behavior of nanofluid under the Lorentz forces, Case Studies in Thermal Engineering 26 (August 2021) 101161.
[15] S. Saranya, Qasem M. Al-Mdallal, Computational study on nanoparticle shape effects of Al_2O_3 -silicon oil nanofluid flow over a radially stretching rotating disk, Case Studies in Thermal Engineering 25 (June 2021) 100943.
[16] Sami Ullah Khan, Alabdan Rana, Abdel-Rahman Al-Qawasmi, Vakkar Ali, Mouna Ben Handa, Iskander Tlili, Bioconvection applications for double stratification 3-D flow of Burgers nanofluid over a bidirectional stretched surface: enhancing energy system performance, Case Studies in Thermal Engineering 26 (August 2021) 101073.
[18] Yi-XiaLi, Taseer Muhammad, Muhammad Bilal, Muhammad Altaf Khan, Ahmadian Ali, Bruno A. Pansera, Fractional simulation for Darcy-Forchheimer hybrid nanoliquid flow with partial slip over a spinning disk, Alexandria Engineering Journal 60 (5) (October 2021) 4787–4796.
[19] Sami Ullah Khan, Nasir Ali, Tahir Mushtaq, Amar Rauf, Sabir Ali Shehzad, Numerical computations on flow and heat transfer of casson fluid over an oscillatory stretching surface with thermal radiation, Therm. Sci. 23 (6A) (2019) 3365–3377.
[20] Muhammad Mubashir Bhatti, S.U. Khan, O.A. Beg, A. Kadir, Differential transform solution for hall and Ion slip effects on radiative-convective Casson flow from a stretching sheet with convective heating, Heat Tran. Asian Res. 49 (2) (2020) 872–888.
[21] Ravinder Kumar, Rakesh Kumar, K. Vajravelu, M. Sheikholeslami, Three dimensional stagnation flow of Casson nanofluid through Darcy-Forchheimer space: a reduction to Blasius/Sakiadis flow, Chin. J. Phys. 68 (December 2020) 874–885.
[22] Muhammad Awais, Muhammad Asif Zahoor Raja, Saeed Ehsan Awan, Muhammad Shoaib, Hafiz Muhammad Ali, Heat and mass transfer phenomenon for the dynamics of Casson fluid through porous medium over shrinking wall subject to Lorentz force and heat source/sink, Alexandria Engineering Journal 60 (1) (February 2021) 1355–1363.
[23] Khalil Ur Rehman, Ebrahem A. Algehyne, Faisal Shahzad, M. El-Sayed, Sherif,Yu-Ming Chu, on thermally corrugated porous enclosure (TCPE) equipped with casson liquid suspension: finite element thermal analysis, Case Studies in Thermal Engineering 25 (June 2021) 100873.
[24] Dzuliana Fatin Jamil, S. Saleem, Rozaini Roslan, Fahad S. Al-Mubaddel, Mohammad Rahimi-Gorji, Alibek Issakhov, Salah UdDin, Analysis of non-Newtonian magnetic Casson blood flow in an inclined stenosed artery using Caputo-Fabrizio fractional derivatives, Comput. Methods Progr. Biomed. 203 (May 2021) 106044.
[25] Salman Saleem, Salman Akhtar, Sohail Nadeem, Anber Saleem, Mehdi Ghalambaz, AlibekIssakhov, Mathematical study of Electroosmotically driven peristaltic flow of Casson fluid inside a tube having systematically contracting and relaxing sinusoidal heated walls, Chin. J. Phys. 71 (2021) 300–311. June.
[26] M.I. Khan, Y.M. Chu, F. Alzahrani, A. Hobiny, Comparative analysis of Al2O3-47 nm and Al2O3-36 nm hybrid nanoparticles in a symmetric porous peristaltic channel, Phys. Scripta 96 (2021), 055005.
[27] J.K. Madhukesh, R. Naveen Kumar, R.J. Punith Gowda, B.C. Prasannakumara, G.K. Ramesh, M.I. Khan, S.U. Khan, Y.M. Chu, Numerical simulation of AA7072-AA7075/water-based hybrid nanofluid flow over a curved stretching sheet with Newtonian heating: a non-Fourier heat flux model approach, J. Mol. Liq. 335 (2021) 116103.
[28] R. Naveen Kumar, R.J. Punith Gowda, J.K. Madhukesh, B.C. Prasannakumara, G.K. Ramesh, Impact of thermophoretic particle deposition on heat and mass transfer across the dynamics of Casson fluid flow over a moving thin needle, Phys. Scripta 96 (2021), 075210.
[29] M.G. Reddy, P. Vijayakumari, L. Krishna, K.G. Kumar, B.C. Prasannakumara, Convective heat transport in a heat generating MHD vertical layer saturated by a non-Newtonian nanofluid: a bidirectional study, Multidiscip. Model. Mater. Struct. 16 (2020) 1669–1689.
[30] G.K. Kumar, A.J. Chamkha, B.C. Prasannakumara, A.M. Jyothi, Exploration of particle shape effect on Cu-H2O nanoparticles over a moving plate: an approach of dual solution, Int. J. Numer. Methods Heat Fluid Flow 30 (2020) 1867–1879.
[31] M. Ijaz Khan, Usman, A. Ghaffari, S. Ullah Khan, Y.M. Chu, S. Qayyum, Optimized frame work for Reiner–Philippoff nanofluid with improved thermal sources and Cattaneo–Christov modifications: a numerical thermal analysis, Int. J. Mod. Phys. B 35 (2021) 2150083.
[32] L. Karthik, G. Kumar, T. Keswani, A. Bhattacharyya, S.S. Chandar, K.B. Rao, Protease inhibitors from marine actinobacteria as a potential source for antimalarial compound, PloS One 9 (3) (2014), e90972.
[33] N.A. Shah, I. Khan, Heat transfer analysis in a second grade fluid over and oscillating vertical plate using fractional Caputo–Fabrizio derivatives, The European Physical Journal C 76 (7) (2016) 1–11.
[34] S. Mondal, N.A. Haroun, P. Sibanda, The effects of thermal radiation on an unsteady MHD axisymmetric stagnation-point flow over a shrinking sheet in presence of temperature dependent thermal conductivity with Navier slip, PloS One 10 (9) (2015), e0138355.
[35] Atangana, D. Baleanu, New Fractional Derivatives with Nonlocal and Non-singular Kernel: Theory and Application to Heat Transfer Model, 2016 arXiv preprint arXiv:1602.03408.
[36] M. Riaz, N. Iftikhar, A comparative study of heat transfer analysis of MHD Maxwell fluid in view of local and nonlocal differential operators, Chaos, Solit. Fractals 132 (2020) 109556.